TERRESTRIAL HEAT FLOW IN UTAH

by
Andrew Henrikson and David S. Chapman

March 2002
University of Utah
Department of Geology and Geophysics
Salt Lake City, Utah

ABSTRACT

New heat flow determinations have been made at 88 sites in Utah using information from oil and gas wells. These sites fill many gaps in the previous heat flow coverage and allow us to better delineate the thermal transition between the Colorado Plateau and the Basin and Range provinces in central Utah.

A thermal relaxation method for correcting oil well bottom hole temperatures (BHTs) was applied to 511 BHTs from 181 wells grouped into 88 sites. Depth to the corrected temperatures ranges from 1 to 5 km. At these depths, the thermal field is minimally affected by surface perturbations caused by topographic relief, microclimate, or near surface (< 500m) hydrologic effects. Fifty-seven new and nearly 2,000 previously determined thermal conductivity values were used with lithologic well logs and regional stratigraphic studies to estimate the thermal conductivity structure for each borehole. Heat flow was determined by calculating a one-dimensional, steady-state geotherm that accounts for volumetric heat production and that minimizes the difference between corrected BHTs and calculated formation temperatures. Errors in heat flow determinations were calculated for clusters of boreholes in the Colorado Plateau and Basin and Range provinces using a Monte Carlo analysis. The probable error of the heat flow was typically 15 percent in the Colorado Plateau compared to 12 percent in the Basin and Range, the primary source of error being the generalizations necessary in prescribing the thermal properties of each borehole.

Previous heat flow studies have determined the mean heat flow for the Basin and Range to be 107 mW^{-2} (standard error of mean (SEM) 8 mW^{-2}) and the mean heat flow for the Colorado Plateau to be 59 mW^{-2} (SEM 4 mW^{-2}). Corresponding mean heat flow values for the new sites are 91 mW^{-2} (SEM 8 mW^{-2})in the Basin and Range and 62 mW^{-2} (SEM 2 mW^{-2}) in the Colorado Plateau. The lateral heat flow gradient from the interior Colorado Plateau to the interior Basin and Range is about 0.3 mW^{-2} km^{-1}. With the addition of these new data, the 75 mW^{-2} contour, which marks the thermal boundary between the Colorado Plateau and Basin and Range, is shifted only slightly but located with greater confidence.

INTRODUCTION

Heat flow studies are critical to understanding many basic geological and geophysical phenomena. The large scale processes that shape the earth leave thermal signatures that may prove crucial to deeper understanding of processes like plate tectonics and crustal magmatism. Heat flow also provides information on the maturation of hydrocarbons, groundwater flow, and displacement rates on faults.

The tectonic evolution of the Colorado Plateau (CP), Basin and Range (B&R), and the Transition Zone (TZ) between them has long been associated with various thermal processes. Explanations for the uplift history of the CP include different modes of plateau uplift, including thermal expansion of the lithosphere due to mantle plumes, subducted ridges and shear heating effects (McGetchin, 1979; McGetchin and others, 1980). McGetchin (1979) also discusses other mechanisms of uplift, such as volumetric expansion due to partial melting, density changes due to dehydration, introduction of volatiles, and density reduction due to iron depletion. Wilson (1973) examined mantle plumes and hotspots and their role in plate tectonics on a global scale, paying special attention to the possibility of the CP uplift being the result of a mantle plume. Anderson and Perkins (1975) examined the irregular patterns seen in the magmatic activity of the CP and attributed them to eddy currents in the large magmatic plume to which the uplift is attributed. Bird (1979) examined the possibility of delamination of the mantle portion of the lithosphere beneath the CP, subsequent replacement of the delaminated section with low density asthenospheric material, causing the observed uplift. Sbar and Sykes (1973) examined the current state of stress fields in the CP and speculated on the tectonic driving forces that would produce them. Thompson and Zoback (1979) studied the idea of lithosphere thinning below the CP due to assimilation of the Farallon plate. Keller and others (1979) examined different seismic velocities and correlated the higher velocities with lower heat flow and vice-versa. The current geological and geophysical state of the CP is summarized in Hunt (1956), Thompson and Zoback (1979), and Stokes (1986).

Many studies have examined the B&R and different aspects of its formation. Lachenbruch (1978) proposed that the high heat flow seen in the B&R could be due to differential strain rates on regional and local scales, and that anomalous conductive heat flow was not necessary to produce the observed heat flow. Hamilton (1987) examined the differing

nature of extension at varying depths within the B&R. The upper crust deforms brittle, the middle deforms through ductile discontinuous shear and the bottom of the crust deforms ductile. Lachenbruch and others (1994) reported mean heat flow values in the northern B&R of 92 ±9 mW^{-2} and mean heat flow in the southern B&R of 82 ±3 mW^{-2}. Lachenbruch and others (1994) also showed that either delamination or magmatic additions could produce the observed results. Klemperer and others (1986) determined that the Moho of the B&R was at a depth of 9-11 s (two-way travel time). Catchings and Mooney (1991) examined velocity contrasts in the B&R of Nevada and concluded that there was a thicker crust in the B&R of 30-35 km thick, up from 22-30 km; that estimate was due to misinterpretation of the Moho in the B&R. Ehlers and Chapman (1999) examined conductive and hydrothermal heat transfer surrounding the Wasatch Fault. Eaton (1982) gives a thorough examination of the geophysical state of the B&R.

Studies of the TZ geology include general regional geology and geomorphology by Hunt (1956) and Stokes (1986). Smith (1978) examined the differences in the crustal thickness between the CP and B&R. Seismic data from the TZ were studied by Loeb (1986) and Pechmann and others (1992) to examine subsurface structures that effect seismic velocities. Wong and Humphrey (1989) defined the state of stress in the CP and TZ. Changes in the stresses in the upper crust of the TZ were examined by Thompson and Zoback (1979), and Zoback and Zoback (1980). Lowry and Smith (1995) determined the effective elastic thickness across the TZ and correlated it to different geophysical characteristics, like heat flow, lithosphereic age, seismic properties, stress orientations, and earthquake focal depths. The TZ plays a crucial role in the geology of Utah because it forms the tectonically active hinge line between the B&R to the west and the CP to the east (Hunt, 1956). Therefore, a better understanding of the thermal state of the TZ will provide greater insight into the tectonic processes that control it.

The thermal state of the B&R, CP and TZ (figure 1) have been the subject of several regional heat flow studies conducted in Utah. These studies include two different methodologies, the shallow borehole or classical method, and the oil and gas well BHT method. The classical method uses high resolution temperature data in relatively shallow holes (< 500 meters) and a tightly constrained thermal conductivity profile. Previous classical heat flow studies in Utah include Roy and others (1968), Sass and others (1971a), Costain and Wright (1973) at various sites around Utah; Reiter and others (1979) in the Four Corners area of the CP;

and Chapman and others (1981) and Clement (1981) in the Escalante Desert, Bodell (1981) and Bodell and Chapman (1982) in the north-central CP; Carrier and Chapman (1981) in southwestern Utah; Bauer (1984) and Bauer and Chapman (1986) at the Stillwater dam site; Powell and Chapman (1990) and Powell (1997) in the TZ; and Moran (1991) at the Jordanelle dam site. Two of the primary difficulties associated with the classical method are perturbation of the temperature field by groundwater flow and topography. The topographic perturbations can be accounted for mathematically (Lachenbruch, 1968; Powell and others, 1988) in the heat flow calculations, but the perturbations due to groundwater circulation are difficult to quantify.

The BHT method utilizes a large body of less reliable and lower precision data found on oil and gas well logs. Once a transient BHT is obtained (from the well log header), it must be corrected to account for the thermal perturbation due to drilling. Thermal conductivity information must be constructed from lithologic or electrical logs or regional stratigraphic studies. Heat flow studies in Utah, based on the BHT method, include Chapman and others (1984) and Keho (1987) in the Uinta Basin, Deming and Chapman (1988a,b) and Deming (1988) in the Utah -Wyoming thrust belt, as well as regional studies of varying extent (Reiter and Mansure, 1982; Eggleston and Reiter, 1984). In addition to the heat flow studies, Willett (1988) modeled the spatial variability in the thermal properties of the Uinta Basin, using stochastic inversion and statistical techniques.

This work presents a number of new heat flow determinations in Utah based on the BHT method mentioned above. New data are combined with previously published Utah heat flow data to create the most complete heat flow map of Utah to date.

This paper starts with a brief review of the geology encountered in the CP, B&R, and TZ. Methods for correcting transient BHTs, assembling thermal conductivity profiles of rocks, and calculating heat flow are described. The resulting heat flow data are then qualitatively compared to previous studies. Finally, the center of the TZ is identified, with the 75 mW^{-2} contour on a map of all existing heat flow data for Utah and comparisons between the new and old datasets are made.

METHODS

Temperature Data

A transient BHT is recorded by a maximum temperature thermometer on an oil or gas well logging tool. Temperatures are least perturbed by drilling at the bottom of the well. As these temperatures are recorded, the length of the shut-in time (t_s) is also recorded as either clock time or the length of time elapsed since the circulation of drilling mud ceased. If multiple transient BHTs are recorded at the same depth in a well, then the thermal relaxation of the well and, in particular, the steady-state BHT can be calculated (Bullard, 1947; Lachenbruch and Brewer, 1959).

The dataset of transient BHTs is freely available and very large, numbering near 100,000 recorded temperatures in Utah alone. The questionable nature of the dataset results from a variety of circumstances including, but not limited to, frequently broken thermometers and misrecording of the data. When examining the log headers, one must be careful, as errant data are not always obvious. Spurious data can be caught at the source by checking to see that, for each well, the temperature at a given depth increases with the shut-in time. Frequently the recorded temperatures for one well-depth are identical for all shut-in times, indicating inadvertent misrecording of data. The wells can also be reconditioned (by recirculation drilling fluid) without mention on the headers. This reconditioning results in widely varying temperature data which appear nonsensical.

The transient BHTs are corrected using methods found in Bullard (1947) and Lachenbruch and Brewer (1959). The method is sometimes referred to as the "Horner plot method" because of the similarity to pressure recovery in a well (Horner, 1951). The thermal recovery method is a convenient and moderately accurate method of estimating formation steady-state temperatures (Deming and Chapman, 1988b; Beck and Balling, 1988; Funnell and others, 1996). The thermal recovery method does have weaknesses, such as minimum shut-in times and certain aspects of drilling that are overlooked. These weaknesses are examined in Luheshi (1983), who mentions that many of the data (mud properties and circulation time) needed to calculate the steady-state BHT are not normally recorded on the well log header.

These problems are avoided in this study by assuming a fixed circulation time and using an approximation which does not rely upon the material properties of the drilling mud. While this approach doesn't eliminate the problem, it does minimize the unseen variability and creates a uniform point from which to correct the transient BHTs.

The transient temperature field ($T(t_s)$) in a well was first described mathematically by Bullard (1947) using the equation

$$T(t_s) = T_\infty - (Q/4\pi k)[Ei(-r^2/4st_s) - Ei(-r^2/4s(t_s+t_c))], \qquad (1)$$

where T_∞ is a steady-state BHT, Q is the line source strength, k is thermal conductivity, Ei is the exponential integral, r is borehole radius, s is system thermal diffusivity, t_s is shut-in time, and t_c is circulation time. When the condition

$$r^2/4st_s << 1 \qquad (2)$$

is met, (1) can be simplified to

$$T(t_s) = T_\infty - (Q/4\pi k)[\ln(t_s/(t_s + t_c)], \qquad (3)$$

as was shown by Bullard (1947). For this study, the portions of equations (1) and (3) that are enclosed in square brackets are referred to as the thermal recovery factor.

Circulation times are almost never recorded in the U.S., but for this study a value of 5 hours is used because it is an intermediate value between the mean of 8 hours and median of 3 hours circulation time found by Scott (1982) in a study of 301 oil wells.

Transient BHTs from a particular depth are plotted against the thermal recovery factor in constructing a thermal recovery plot (figure 2). A linear least-squares fit is applied to the plotted transient BHTs and the resulting line is extrapolated to the T-intercept, which represents infinite shut-in time and therefore the steady-state formation temperature. Thermal recovery plots that used two transient BHTs are called two-point data and the thermal recovery plots that used three or more data points are called three-point data.

The slope of the least-squares line on the thermal recovery plot also provides information about the area being examined. The greater the slope, the higher the rate of recovery and therefore, the greater the initial perturbation. For example, in figure 2, the wells State of Utah "L" and State of Utah "K" both have very high rates of thermal recovery for their respective depths. These are typical of the Great Salt Lake area, and reflect the high thermal gradients observed beneath the Great Salt Lake.

Unfortunately, the exponential integral, or exact, solution (equation (1)) requires information on the thermal diffusivity of the borehole-country rock system. Thermal diffusivity is seldom measured and variability in the factors involved in calculating the system thermal diffusivity can cause large unknown variations in the thermal recovery factor. The variation in thermal recovery factor causes corresponding errors in the calculated steady-state temperature. With a fixed diffusivity, for example, the thermal recovery factor from the exact solution was shown to differ by as much as 12 percent from the thermal recovery factor of the logarithmic approximation (3) for the data used in this study (figure 3 A). Fortunately, this rather large shift in the thermal recovery factor alters the slope of the thermal recovery curve, but has only a small affect (1-2 percent) on the final calculated steady-state temperature (figure 3 B). The difference between the approximation and exact solution decreases as the shut-in time increases. This convergence over time of the exact solution and the approximation, and the high degree of variability introduced by the diffusivity term in the exact solution, provides adequate reason to use the approximation.

Equation (3) thus provides a convenient basis for estimating a steady-state BHT if two or more transient BHTs are measured at a given depth. In many wells, unfortunately, only a single transient BHT is determined. We now investigate empirical predictions of the thermal recovery rate in order to extract steady-state BHT estimates from single point data.

Wells are grouped according to diameter because the diameter appears to have a first-order effect on the rate of thermal recovery. The oil and gas wells are organized into three groups: 150-154 mm (5.9-6.0 in) diameters are labeled as 150 mm, 180-250 mm (7.1-9.8 in) are labeled as 205 mm, 311-365 mm (12.2-14.4 in) are labeled as 311mm, and 365-475 mm (14.4-18.7 in) wells are labeled as 445 mm. These labels reflect the diameters of the majority of the boreholes in any specific group.

When oil wells are drilled, the first section to be drilled is the widest. As the well

deepens the diameter of the hole decreases. Many of the well logs are run during the breaks in drilling when the drill bits are being changed or replaced. This narrowing of the well is important to remember when considering the location and likely role of a well of a given diameter. For example, the narrowest (150 mm, 5.9 in) holes are generally the very deepest sections of oil or gas wells, although they also are used for shallow exploration. As a result of the limited role of the 150 mm (5.9 in) diameter wells, they are less common than the other wells and only 29 of them are included in this study. The sizes 205 and 311 mm (8.1 and 12.2 in) are more common, with 140 and 60 wells in each group, respectively. Oddly, the 311 mm (12.2 in) wells had very little near-surface data, probably the result of them being used as a second-stage for still larger diameter wells. The largest wells (445 mm [17.5 in] and larger) are relatively rare and almost all are very shallow, probably because they are used only as a first stage for very deep wells.

Depth-dependent correction equations for each of the above mentioned diameter groups were determined by graphing slopes from individual thermal recovery plots against their respective depths (figure 4). The data presented suggest a nonlinear trend that was quantified by fitting a quadratic function to the dataset using the least-squares method. The best-fit quadratics for the two-point data show a slight systematic shift to the right of the three-point data best fit line. The quadratic function gives a predicted rate of thermal recovery for any individual well as a function of depth. From this rate of recovery, the formation steady-state temperature can be estimated for wells with a single temperature depth measurement.

The criterion (2) for using the approximation (3) requires the shut-in times of the wells to be of a required minimum duration. The minimum shut-in time depends on the diameter of the well. For wells with diameters of 445 mm (17.5 in), 311 mm (12.2 in), 205 mm (8.1 in) and 150 mm (5.9 in), minimum shut-in times are 8, 7, 5 and 4 hours respectively (Funnell and others, 1996). In the context of the condition (2), the ratios of well diameter and shut-in time are not all equal. However, in order to make use of the data from larger diameter oil wells, the minimum shut-in time standard had to be reduced, relative to the well diameter. The error in the calculated steady-state BHT associated with these minimum shut-in times can be as large as 5 percent, but is usually less (Funnell and others, 1996). This criterion effectively removed the 445 mm wells from this study because none of the wells had sufficient shut-in times.

The quadratic trendlines are constrained to have a zero intercept based on the assumption

that the drilling fluid has the same temperature as the ground surface at the drilling site, and are of the form

$$A = az + bz^2 , \qquad (4)$$

where A is the slope of the thermal recovery plot and z is depth (table 1). The result is a predicted depth-dependent rate of recovery for any well that has been shut in for an adequate period of time as described above.

The deviations of the two-point data from the curve compared to the deviation of the three-point data from the curve were quantified by calculating root mean square (rms) residuals (table 2). As expected, the three-point data, being more tightly constrained than the two-point data, better fit the trendline than the two-point data. The purpose of this analysis was to determine if the two-point data and the three-point data were sufficiently similar to be used together. As expected, the less constrained two-point data exhibited greater scatter, but the best fit curves of both the three and two-point data are similar (figure 4). The improvement in the curve-fit of the data from two-point to three-point was not uniform for the different well groups. The rms residual for the smallest wells improved by about 5°C (41°F), for the 205 mm (8.1 in) wells about 4°C (39°F), for the 311 mm (12.2 in) wells by 3°C (37°F) (table 2).

A common problem when using the thermal recovery method is a lack of the multiple transient BHTs at a single depth required to construct a thermal recovery plot. The majority of the data in this study have multiple transient BHTs and thus yield heat flow values directly. An additional 64 heat flow values were obtained in wells having single transient BHTs at a given depth by employing the correction equations (table 1). The search for these additional data was based on geographic density of data points for any given region, with the greatest attention being paid to regions with little or no temperature-depth data. The additional data improved the spatial coverage of the data, but there are regions of Utah where oil and gas wells are absent. Therefore, there are large regions with few deep thermal data.

A group of 447 measured transient BHTs from 117 different wells were initially used in the thermal recovery method to determine 174 new, corrected BHTs. The ratio of transient BHTs to corrected BHTs is approximately 3:1. Because the thermal recovery method relies on a best-fit line to determine the corrected BHT, the 3:1 ratio further constrains the best-fit line,

resulting in a greater degree of confidence in the corrected BHTs. The data from the above mentioned 110 corrected BHTs were then used to create the correction equations. Using the correction equations, an additional 64 uncorrected BHTs, which brought the total uncorrected BHTs to 511, in 64 separate wells were corrected to bring the total number of corrected BHTs to 240 in a total of 181 different wells.

All of the temperature-depth data generated by this study are plotted in figure 5. The majority of the oil and gas wells examined in Utah have average thermal gradients between 18 and 45°C km^{-1} (0.99 and 2.5°F/100 ft). This range reflects the various tectonic settings across the state, from the cool interior of the CP (Bodell, 1981) to the relatively hot Great Salt Lake area. The high thermal gradients below the Great Salt Lake area were initially viewed with skepticism. However, because of the uniform nature of the geothermal gradient in the area, the Great Salt Lake is treated as a geographically bounded anomaly and the wells therein are kept separate from the other groups of wells.

The surface temperatures (T_0) used in the heat flow calculation were determined by taking the average annual air temperature of a nearby weather station and adjusting for air-ground temperature differences and elevation. We assumed that ground temperature is on average 2.9°C (37.2°F) warmer than the air temperature and that temperature decreases with elevation at a rate of -7°C km^{-1} (-0.4°F/100 ft) (Powell and others, 1988).

Thermal Conductivity Measurements

Thermal conductivity measurements were made on 57 rock samples from five different formations (table 3). Hand specimens greater than 12 cm (4.7 in) in diameter and thicker than 5 cm (2 in) from the Simonson Dolomite, Sevy Dolomite, Guilmette Formation and Hermosa Group, were measured with a TK04 line source instrument using methods outlined in Sass and others (1984). The Hermosa Shale was measured, in crushed form, in cells on the University of Utah divided bar using equipment and methods outlined in Sass and others (1971a) and Bodell (1981). Results are shown in table 3.

The number of samples collected for a formation reflects the magnitude of the thermal resistance (thickness/thermal conductivity) of the formation and thus the overall impact of the formation on the heat flow calculation. Therefore, the greater the thermal resistance of the

formation, the more times we sampled the unit. All measurements from an individual formation were averaged to account for the heterogeneities inherent in the rocks. However, the anisotropy and friable nature of shale makes reliable laboratory measurements difficult. Gallardo and Blackwell (1999) showed that the in-situ measured thermal conductivity of shale can be almost half that of the laboratory measurements of the same formation. Unfortunately, the methods described in Gallardo and Blackwell (1999), whereby conductivites are inferred from the ratio of thermal gradients through multiple formations in a single well, require resources that were unavailable for this project.

The proximity of nearest-neighbor wells, however, affords a different kind of field calibration for thermal conductivity of shales. We consider pairs of heat flow sites which penetrate the Mancos Shale with nearest-neighbor sites which do not encounter the Mancos. The matrix conductivity of the Mancos Shale was adjusted so that these sets of proximal sites would have identical heat flow. The matrix thermal conductivity values necessary to produce equivalent heat flow values are given for each well in table 4. A weighted mean of matrix conductivity based on the percentage of the stratigraphic column occupied by the Mancos Shale resulted in a matrix conductivity of 1.7 W m^{-1} K^{-1} , which in turn resulted in an average in-situ thermal conductivity of 1.5 W m^{-1} K^{-1}. These values are consistent with the shale conductivity values reported in Gallardo and Blackwell (1999). Heat flow calculations that involved the Mancos Shale (laboratory measured at 2.48 W m^{-1} K^{-1}) were recalculated using a matrix thermal conductivity of 1.7 W m^{-1} K^{-1} (table 4).

This study also makes extensive use of previously published thermal conductivity measurements of rocks from Utah (Bodell, 1981; Carrier and Chapman, 1981; Keho, 1987; Deming, 1988; Deming and Chapman, 1988b; Moran, 1991; and Powell, 1997). For formations for which there are no measured or published conductivity data, values were used from measurements of lithologically similar formations. These are referred to as assumed thermal conductivity values.

Matrix thermal conductivities in table 3 are converted to in situ conductivity by accounting for porosity and temperature effects. Thermal conductivity (k) of a porous medium can be expressed as

$$k = k_s^{(1 - \phi)} k_w^{\phi}, \qquad (5)$$

where k is the in situ thermal conductivity, ϕ is porosity, k s is conductivity of the solid matrix, and k w is conductivity of the pore-filling fluid, in this case water. The porosity values used in this study are calculated using exponential compaction trends

$$\phi_z = \phi_0 e^{(-z/d)}, \quad (6)$$

described in Sclater and Christie (1980), Rieke and Chilingarian (1974), and Bond and Kominz (1984), where ϕ z is porosity at depth (z), ϕ 0 is porosity at zero depth and d is a compaction constant.

Surface porosity varied based upon lithology and local geology. Typical values measured for ϕ 0 were 0.4 for valley fill, 0.08 for limestones and dolomites, and 0.22 for sandstone (Bodell, 1981; Carrier and Chapman, 1981; Keho, 1987; Deming, 1988; Deming and Chapman, 1988b; and Powell, 1997). The porosity of the shale samples could not be measured because the shale lacked sufficient cohesion to survive water saturation intact. These surface porosity values reflect burial, compaction, and subsequent exhumation (figure 6). The compaction curves (figure 6) (Sclater and Christie, 1980) were used to determine shale porosity. Porosity values measured by previous workers were used in conjunction with those in table 3 to determine the surface porosity values used in the model. Current surface porosity reflects the maximum depth of burial, and subsequent exhumation, assuming no reopening of pores due to exhumation. However, some porosity values were adjusted for the near-surface ($\leq$500 m) increase in porosity of uplifted CP strata described in Jarrard and others (1999). Based on measured porosities, the sediments of the CP were assumed to have been exhumed 3,500 m (11,500 ft) and the older rocks in the B&R were exhumed 3,000 m (9,840 ft). These empirically derived porosity values agree reasonably well (±10 percent) with the laboratory measured values of Powell (1997) and Bodell (1981).

Adjustment of the matrix conductivity (k) values for temperature was accomplished by using the relation given by Chapman and Furlong (1992)

$$k = k_{20} [1/(1 + 0.0005 (T))], \quad (7)$$

where k_{20} is the matrix conductivity at 20°C and T is the temperature in degrees Celsius. The total effect of the temperature adjustment is less than 1 percent, which falls within the expected bounds of error for this study.

The conductivity of the pore water was calculated using the polynomial, relating temperature to conductivity, given by Deming and Chapman (1988b) based on data from Touloukian and others (1970). No adjustments were made for the salinity of the pore water.

Heat production in the rocks of the CP and B&R is a minor factor in calculating heat flow. Values of 0.5 $\mu W\ m^{-3}$ were assigned to sandstone and limestone strata, 1.0 $\mu W\ m^{-3}$ to valley fill, and 1.8 $\mu W\ m^{-3}$ to shale, based on values from Funnell and others (1996) and Rybach (1986). The heat production of the rock layers involved in the calculation typically contributed 5 percent or less of the total surface heat flow.

When making regional heat flow calculations it is not always practical to sample rocks for thermal conductivity measurements every few vertical meters in every borehole as suggested by Chapman and others (1984). The bulk of the conductivity data that are available are organized by geological groups, formations, and members. With data in this structure, thermal conductivity profiles are created by determining the most likely stratigraphy for a borehole, or cluster of boreholes, down to the required depth, and by applying the thermal conductivity data to the stratigraphic profile. Ideally this is accomplished using lithological well logs. However, few such logs are available for oil and gas wells. More prevalent are SP and neutron log interpretations of the lithology, typically given as percentages of sand, limestone, or shale. Because the thermal conductivity data are based on stratigraphic units, this end-member knowledge is not an adequate substitute for knowledge of the actual stratigraphy.

Although the conductivity of a given formation has been shown to vary up to 25 percent laterally, as in the case of the Navajo-Nugget sandstone, with the exception of Chapman and others (1984) and Willett (1988) lateral variation of thermal conductivity within a formation has not been addressed in detail. The structure of the rocks and thicknesses of the beds used in the calculations are based on regional stratigraphic studies (Hintze, 1988) and, whenever possible, lithology logs. The possible errors in conductivity that are outlined above are analyzed using a Monte Carlo error analysis discussed later.

Computation of Present-Day Surface Heat Flow

The variation of temperature with depth (T(z)) for steady-state heat conduction through a horizontally layered Earth that includes heat production is given by

$$T(z) = T_0 + \sum_{i=1}^{n}[(q_{i-1}\Delta z_i)/k_i - (A_i \Delta z_i^2)/2k_i], \quad (8)$$

where

$$q_i = q_{i-1} - A_i \Delta z_i \quad (9)$$

T_0 is the surface temperature; q_i is the heat flow into the base of layer i; q_{i-1} is the heat flow out of the top of the ith layer; Δz_i, k_i, and A_i are the thickness, thermal conductivity and heat production, respectively, for the ith depth interval in a well.

Equation (8) leads directly to the "Bullard" method of calculating heat flow (Bullard, 1947) assuming negligible heat production and therefore constant q_i. This simplification results in

$$T(z) = T_0 + q_0 \sum_{i=1}^{n} \Delta z_i/ki, \quad (10)$$

where q_0 is the surface heat flow. In practice, heat flow is determined from the Bullard method and equation (10) as the slope of a line when temperature is plotted against summed thermal resistance ($\Delta z_i/\Delta k_i$).

In this study, equations (8) and (9) were used for the primary heat flow calculations. Steady-state BHT data are combined with ground surface temperatures, and thermal conductivity data as input to equations (8) and (9). This is accomplished using a spreadsheet which creates a temperature-depth profile for each heat flow site using equations (8) and (9), based on heat production, porosity, temperature effects, steady-state BHT, and thermal conductivity data. In equations (8) and (9), once the layer thicknesses, heat production and thermal conductivity profile have been determined, a temperature at any given depth can be calculated by assuming a

surface heat flow. In this calculation the only value that is not predetermined is the heat flow, so by iterating through various surface heat flow magnitudes, alteration of the calculated geothermal gradient is possible. An optimum surface heat flow value is found that minimizes the differences between a calculated temperature for the approximate depth and the corrected BHT.

Wells that were within 0.1° longitude and 0.1° latitude (about 11 km; 6.8 mi) of each other or in an area of uniform geology were grouped and treated as a single location. This clustering resulted in an increase in the number of corrected BHTs used in each heat flow calculation.

Error Analysis

The uncertainty in heat flow values determined by the "Bullard" method depends on uncertainties in formation thicknesses and thermal conductivities, surface temperature, and corrected BHTs. The effects of these errors on the heat flow calculation were evaluated using a Monte Carlo analysis and equation (10).

In the Monte Carlo analysis, perturbations were applied to thermal conductivity, formation steady-state temperatures, mean surface temperature, and the positions of the rock layer interfaces which govern layer thicknesses for as many as 10 formations (table 5). These parameters were perturbed in each heat flow realization using a random number generator that produces values in a Gaussian distribution with a mean of zero and a variance of one. We scaled the magnitude of each perturbation in a realization by multiplying each random number by the estimated variability for that specific parameter.

Thermal conductivity was perturbed according to the magnitude of the standard deviation of the thermal conductivity of each formation. If a formation in the stratigraphic column was not measured in the lab and there were no preexisting thermal conductivity data for it, a standard deviation of 0.15 of its assumed conductivity was assigned. The standard deviation of the mean, annual surface temperature was assumed to be 1°C, based on meteorological records that typically represent 100 years of data. The corrected BHTs were randomized by 10 percent, a magnitude based on a likely error associated with the thermal recovery method.

Monte Carlo analyses are presented here for two sites, one each from the CP and B&R (figure 7 and figure 8, respectively). Each analysis produced a scatter plot of temperature

difference (T(z)-T 0) versus thermal resistance and a histogram showing the distribution of computed heat flow values per 1,000 realizations.

For the area on the CP, the analysis was performed on the well "Salt Valley #1" (figure 7). The corrected BHT is 78.3°C (172.9°F) at a depth of 3,448 m (11,312 ft), the assumed surface temperature is 14.7°C and the mean value of the summed thermal resistance is 1,056 m^2°CW^{-1}, yielding a deterministic heat flow value of 61 *m*W $^{-2}$. The Monte Carlo simulation produced extreme perturbations of 37 and 94°C (99 and 201°F) for T(z)-T_0 and 785 and 1,420 m^2 KW^{-1} for the summed thermal resistance. Heat flow values for these extremes vary from 35 to 90 *m*W m^{-2}. The standard deviation of the 1,000 realizations for this well is 8.7 *m*W $^{-2}$, or 15 percent of the mean heat flow of 60 *m*W $^{-2}$.

For the area on the B&R, the analysis was performed on the well "State of Utah N#1" (figure 8) the corrected BHT is 111°C (232°F) at a depth of 2,000 m (6,562 ft), the assumed surface temperature is 13.9°C (57.0°F) and the mean value of the summed thermal resistance is 773 m^2 °CW^{-1} , yielding a deterministic heat flow value of 127 *m*W $^{-2}$. The Monte Carlo simulation produced extreme perturbations of 80 and 117°C (176 and 243°F) for T(z)-T_0 and 600 and 1,200 m^2 KW^{-1} for the summed thermal resistance. Heat flow values for these extremes vary from 75 to 175 *m*W $^{-2}$. The standard deviation of the 1,000 realizations for this well is 15.7 *m*W m^{-2}, or 12 percent of the mean heat flow of 127 *m*W $^{-2}$.

DISCUSSION

The thermal resistance method relies on temperature data and thermal properties to compute heat flow. Each well was not necessarily restricted to a single corrected BHT at a single depth. Therefore, in some cases, a temperature-depth series could be used to constrain the geothermal gradient and reduce random error. Each iteration of the spreadsheet served to minimize the differences between the corrected BHT data and the calculated temperature for that depth. In an attempt to reduce the overall random error, wells were grouped together, based on distance apart and continuity of local geology. Generally, the wells grouped together are within 11 km, although that range was extended or restricted based on the uniformity of local geology. The benefit of grouping is that the random error associated with the corrected BHTs is more likely to cancel out with the increase in the number of corrected BHTs used for each heat flow

calculation.

The new heat flow values for Utah are plotted in figure 9 and consist of two numbers. The upper bold number is the heat flow for that well or cluster of wells. The lower of the two numbers represents the number of transient BHTs used to make the heat flow determination. The larger the number of transient BHTs used in the thermal recovery plots, and therefore the thermal gradient calculations, the greater the confidence in the calculated thermal gradient.

Figure 10 shows the updated heat flow data for Utah. The bold numbers with solid circles represent new heat flow determinations from this study. Plain numbers with open circles represent heat flow values from previous studies. In some cases a number of heat flow values from previous studies have been averaged to facilitate legibility. The number in parentheses indicates the number of heat flow values that were averaged.

The overall pattern of the new heat flow map is higher values in the west and lower values in the east, although there are exceptions. The new data presented in figure 9 yield an average heat flow for the B&R of 91 mW^{-2} (standard error of the mean (SEM) 8 mW^{-2}). Previous studies (Roy and others, 1968; Costain and Wright, 1973; Reiter, and others, 1979; Carrier and Chapman, 1981; Chapman, and others, 1981, Eggleston and Reiter, 1984; Moran, 1991; Powell, 1997) yield an average heat flow value of 107 $mW\ m^{-2}$ (SEM 8 $mW\ m^{-2}$) for the B&R. Due to the fact that the two SEM do overlap, these values can not be considered statistically different. Some of the previously existing heat flow data in the B&R came from studies conducted for geothermal resources exploration. These geothermal studies produced some extremely high (500 - 3,000 mW^{-2}) heat flow values that were not included in the calculation of the mean of previously published data. However, it is likely that the data, none the less, were biased toward higher values and the mean of that data is not representative of the entire region. In contrast, BHT values are from oil and gas wells drilled in sedimentary basins. These values are likely to be cooler due to the depression of the geotherms in the sedimentary basin (Gallardo and Blackwell, 1999; Sclater and Christie, 1980), and more uniform than those drilled for geothermal exploration. The mean of all known heat flow data for the B&R, excepting the geothermal exploration data, is 105 $mW\ m^{-2}$, SEM 5 $mW\ m^{-2}$.

The average heat flow in the CP as determined by this study is 62 $mW\ m^{-2}$ (SEM 2 $mW\ m^{-2}$). Previous studies (Costain and Wright, 1973; Reiter and others, 1979; Bodell, 1981; Bodell and Chapman, 1982; Reiter and Mansure, 1982; Eggleston and Reiter, 1984; Powell, 1997) yield

an average heat flow value of 59 *m*W m^{-2} (SEM 4 *m*W m^{-2}) for the CP. The overlap in the SEM of these mean values indicates that they are not statistically different. The mean of all known heat flow data for the CP in Utah is 60 *m*W m^{-2} with a SEM of 1 *m*W m^{-2}.

An ideal comparison between two sets of heat flow data would be point by point, comparing heat flow determinations in a single borehole or oil well by multiple studies. Unfortunately, no such groupings exist. Instead, a nearest-neighbor approach is used. Scatter plots (figure 11) show the nearest-neighbor comparison between the old and new data from figure 10. In the B&R (figure 11 A) the previously published heat flow values are slightly higher than the new data, indicated by the slope of 1.03 of the least-squares best fit line. In figure 11 B the trend is slightly higher heat flow values from this study compared to the previously published data in the CP, indicated by the slope of 0.92 of the least-squares best fit line. It should be noted that the removal of the outliers seen in figure 11B does not change the slope of the best-fit line appreciably. The scatter seen in the data does not increase with increased distance from the nearest-neighbor. This is not surprising considering the difficulty encountered in contouring heat flow data. These scatter plots are consistent with the provincial means discussed earlier in this section.

There are some interesting aspects to the new data (figure 9), starting from the north: two data points which straddle the TZ, representing 43 transient BHTs, which average 75 *m*W $^{-2}$, are marginally higher than the surrounding heat flow values. These are located on the Utah-Wyoming thrust belt at approximately 111.3°W, 41.3°N. The heat production in the thrust sheet could account for most of this modest increase in heat flow, provided the thrust sheet was 3 km thick when emplaced and produces heat at a rate of 2 µW m^{-3} (Deming, 1988). This heat production rate is slightly higher than any used in this study, but is not unreasonable and would explain roughly 6 *m*W m^{-2} of the observed difference in heat flow.

Farther south and astride the TZ east of Nephi around 111°W, 39.6°N, there are two new values of 54 and 72 *m*W m^{-2} representing 18 transient BHTs which are in close proximity to two other values of 88 and 89 *m*W m^{-2}. The two high values are from Eggelston and Reiter (1984) and are based on BHT data. However, for their thermal conductivity data, they assigned the average of previously published thermal conductivity values, corresponding to the lithologies encountered by the lithology logs. Most of the thermal conductivity data for rocks in Utah that now exist did not exist in 1984, so the values they were employing were not from rocks in Utah.

They used these foreign values in their calculations instead of an actual formation-based conductivity structure. Eggelston and Reiter (1984) estimate their error to be 10 percent to 15 percent. This would suggest a minimum heat flow of 76 *m*W m^{-2}. Assuming an error of 12-15 percent shown by the Monte Carlo analysis, the values from this study could be as high as 63 and 88 *m*W m^{-2}. While the probable error bars do overlap, the disagreement between the 54 *m*W m^{-2} and the previously published values can also be explained through the foreign nature of the thermal conductivity values used by Eggelston and Reiter (1984).

The thermal transition from the CP to the B&R has traditionally been defined as the 75 *m*W m^{-2} contour (Powell, 1997) (figure 10). However, there is a great deal of scatter in the heat flow determinations. This degree of scatter is common in heat flow studies and is a primary reason that data from regional heat flow studies are rarely contoured. The position of the 75 *m*W m^{-2} contour that delineates the TZ is seen in figure 10 as the solid curved line running from the Idaho border near 111°W longitude to the Nevada border near 38°N latitude.

The transition in heat flow between the B&R and CP reflects a number of factors. When a warm province abuts a colder province, the zone that thermally separates them will blur as heat diffuses laterally from higher to lower temperature rocks. Differences in thermal conductivity cause refraction of heat from the lower to higher conductivity. For example, the thicker, cooler granitic crust that supports the CP (Keller and others, 1979; Thompson and Zoback, 1979; Benz and others, 1990) probably acts to draw heat away from the edge of the warmer B&R. This theory is supported by the velocity profiles found in Benz and others (1990). Using a simple thermal length calculation, the warm thermal signal from the B&R would have conducted 44 km (27 mi) into the cooler CP in the 15 Ma since the extension began. This length scale coincides fairly well with the 50 km (31 mi) average width of the thermal transition.

Another process that can affect the surface heat flow is volcanism. At first glance, volcanism seems to appear in Utah as modest heat flow highs around the Marysvale area. Using a thermal-length argument presented in Lachenbruch and others (1976), we have determined that the apparent heat flow highs in the area of the Marysvale volcanics are not related to the volcanic activity of the last 15-30 Ma. The activity was too small in scale and too long ago to leave any discernible signal.

Also important to remember are mechanisms that may serve to focus or disperse heat in certain areas. One candidate source is near-surface groundwater flow. For example, Chapman

and others (1984), Keho (1987), and Willett (1988) describe the effects of near-surface groundwater effects on the heat flow in the Uinta Basin. The CP and B&R both have relatively porous rocks in positions of relatively high relief that can result in strong groundwater circulation.

Topographic relief was not considered a factor in this study because the topographic relief was generally small, relative to the depth of measurement and the horizontal distance to the depth of measurement (Lachenbruch, 1968).

The thermal transition in figure 10 generally agrees with previously published CP-B&R thermal transition zones (Bodell, 1981; Blackwell and Steele, 1992; Lowry and Smith, 1995; Powell, 1997). Blackwell and Steele (1992) mapped regional heat flow and interpolated the transition. Their estimation is surprisingly close to the TZ determined in this study, especially considering the sparse data from the region at the time. Lowry and Smith (1995) examined the relationship between the elastic thickness of the TZ and heat flow, seismicity and focal mechanisms. Integrating these data resulted in a transition zone that is located to the east of the geomorphic transition. Lowry and Smith (1995) do not map their transition. Instead, they present a series of west to east cross sections, showing the geophysical properties across the Transition Zone that they investigated in that area. Their series of cross sections does follow the same trend that this study found. The Powell (1997) thermal TZ in southern Utah matches the thermal transition produced by this study, but it diverges to the east near the Uinta Basin, probably because of sparse data.

The Monte Carlo error analysis provided probable bounds for the error associated with the calculations performed, based on rock layer interfaces, known errors in thermal conductivity, and temperature gradients. The errors employed in the calculation were as realistic as possible, and sometimes intentionally overestimated to examine worst-case scenarios. However, the errors used may in fact be much too small and future studies could further refine the TZ. The heat flow in Utah is represented to within 15 percent by the data presented here.

CONCLUSIONS

New heat flow determinations have been made at 88 sites in Utah using information from

oil and gas wells. These sites fill many gaps in the previous heat flow coverage and allow us to better delineate the thermal transition between the CP and the B&R in central Utah. Thermal gradients are determined from oil and gas well steady-state BHTs and weather station data. Measured thermal conductivity for five formations and previously published data from approximately 80 additional Utah formations were used in the calculations.

The new heat flow values were combined with previously published data to create a heat flow map for Utah and to define the thermal TZ more accurately. The following conclusions were reached:

1. The mean heat flow of newly determined sites for the B&R in Utah is 91 *m*W m^{-2} with a standard error of the mean (SEM) of 8 *m*W m^{-2}. This heat flow for the B&R is somewhat lower than determined in previous studies, many of which were geothermal exploration projects that focused on anomalously high heat flows. The mean of all known heat flow data for the Utah B&R (excluding geothermal resource exploration) is 105 *m*W m^{-2} with SEM 5 *m*W m^{-2}.

2. The mean heat flow for the CP in Utah is 62 *m*W m^{-2} with SEM 2 *m*W m^{-2}. This heat flow for the CP is not significantly different from previous studies. The mean of all known heat flow sites on the CP is 60 *m*W m^{-2} with SEM 1 *m*W m^{-2}.

3. The thermal transition for B&R to CP is better delineated. It is 50 to 100 km east of the geomorphic transition. The systematic changes in the heat flow values from east to west across Utah reflect the different tectonic provinces contained therein and 15 to 20 Ma of conductive heat transport between them.

4. Monte Carlo analyses indicate that the heat flow values determined by the BHT method are reliable to 12-15 percent, provided the thermal conductivity structure is well constrained.

The tectonic differences between the B&R and CP are manifested in numerous ways, not least of which is a contrast in heat flow. The transition between the two are marked by the

geomorphic, stratigraphic, and tectonic transitions. Geomorphology, stratigraphy, and tectonics all affect the thermal transition in some way, but a systematic lateral heat flow gradient of about 10 *m*W m^{-2} per degree longitude is a generally observable characteristic.

REFERENCES

Anderson, O.L., and Perkins, P.C., 1975, A plate tectonic model involving non-laminar asthenospheric flow to account for irregular patterns of volcanism in the southwest United States: Physical Chemistry Earth, v. 9, p.113-122.

Bauer, M.S., 1984, Heat flow at the Upper Stillwater dam site, Uinta Mountains, Utah, Salt Lake City, University of Utah, M.S. thesis, 94 p.

Bauer, M.S., and Chapman, D.S., 1986, Thermal regime at the Upper Stillwater dam site, Uinta Mountains, Utah: implications for terrain, microclimate and structural corrections in heat flow studies: Tectonophysics, v. 128, p. 1-20.

Beck, A.E., and Balling, Niels, 1988, Determination of virgin rock temperatures, *in* Haenel, Ralph, Rybach, Ladislaus, and Stegena, Lajos, Handbook of Terrestrial Heat Flow Density Determination: Kluwer Academic Publishers, Dordrecht, 59-85 p.

Benz, H.M., Smith, R.B. and Mooney, W.D., 1990, Crustal structure of the Northwestern Basin and Range province from the 1986 program for array seismic studies of the continental lithosphere seismic experiment, Journal of Geophysical Research, v. 95, p. 21823-21842.

Bird, P.H., 1979, Continental delaminating and the Colorado Plateau: Journal of Geophysical Research, v. 84, p. 7561-7571.

Blackwell, D.D., and Steele, J.L., 1992, Geothermal map of North America: Boulder, Colorado, Geological Society of America, scale 1:5,000,000.

Bodell, J.M., 1981, Heat flow in the north-central Colorado Plateau, Salt Lake City, University of Utah, M.S. thesis, 134 p.

Bodell, J.M., and Chapman, D.S., 1982, Heat flow in the north-central Colorado Plateau, Journal of Geophysical Research, v. 87, p. 2869-2884.

Bond, G.C., and Kominz, M.A., 1984, Construction of tectonic subsidence curves for the early Paleozoic miogeocline, southern Canadian Rocky Mountains; implications for subsidence mechanisms, age of breakup, and crustal thinning, Bulletin of the Geological Society of America, v. 95, p. 155-173.

Bullard, E.C., 1947, The time taken for a borehole to attain temperature equilibrium, Monthly Notices of the Royal Astronomical Survey, Geophysical Supplement, v. 5, p. 127-130.

Carrier, D.L., and Chapman, D.S., 1981, Gravity and thermal models for the Twin Peaks volcanic center, southeastern Utah: Journal of Geophysical Research, v. 86, p.10287-10302.

Catchings, R.D., and Mooney, W.D., 1991, Basin and Range crustal and upper mantle structure, northwest to central Nevada: Journal of Geophysical Research, v. 96, p. 6247-6267.

Chapman, D.S., Clement, M.D., and Mase, C.W., 1981, Thermal regime of the Escalante Desert, with analysis of the Newcastle geothermal system: Journal of Geophysical Research, v. 86, p. 11735-11746.

Chapman, D.S., and Furlong, K.P., 1992, Thermal state of the continental lower crust, *in* Fountain, D.M., Arculus, R. and Kay, R.W., editors, Continental Lower Crust, v. 23, New York, Elsevier, p. 179-199.

Chapman, D.S., Keho, T.H., Bauer, M.S., and Picard, M.D., 1984, Heat flow in the Uinta Basin

determined from bottom hole temperature data: Geophysics, v. 49, p. 453-466.

Clement, M.D., 1981, Heat flow and geothermal assessment of the Escalante Desert, part of the Oligocene to Miocene volcanic belt in southwestern Utah: Salt Lake City, University of Utah, M.S. thesis, 118 p.

Costain, J.K. and Wright, P.M., 1973, Heat flow at Spor mountain, Jordan Valley, Bingham and La Sal, Utah: Journal of Geophysical Research, v. 78, p. 8687-8698.

Deming, David, 1988, Geothermics of the thrust belt in north-central Utah: Salt Lake City, University of Utah, Ph.D. thesis, 197 p.

Deming, David, and Chapman, D.S., 1988a, Inversion of bottom-hole temperature data: The Pineview field, Utah-Wyoming thrust belt: Geophysics, v. 53, p. 707-720.

--- 1988b, Heat Flow in the Utah-Wyoming thrust belt from analysis of bottom hole temperature data measured in oil and gas wells: Journal of Geophysical Research, v. 93, p. 13657-13672.

Ehlers, T.A., and Chapman, D.S., in press, Normal fault thermal regimes: Conductive and hydrothermal heat transfer surrounding the Wasatch Fault, Utah: Tectonophysics.

Eaton, G.P., 1982, The Basin and Range province: Origin and tectonic significance, Annual Reviews of Earth and Planetary Sciences, v. 10, p. 409-440.

Eggleston, R.E., and Reiter, Marshall, 1984, Terrestrial heat-flow estimates from petroleum bottom- hole temperature data in the Colorado Plateau and eastern Basin and Range province, Bulletin of the Geological Society of America, v. 95, p. 1027-1034.

Fenneman, N.M., 1946, Physical divisions of the United States (map): United States Geological Survey, scale 1:7,000,000.

Funnell, Robert, Chapman, D.S., Allis, R.G., and Armstrong, P.A., 1996, Thermal State of the Taranaki Basin, New Zealand: Journal of Geophysical Research, v. 101, p. 25197- 25215.

Gallardo, J.A., and Blackwell, D.D., 1999, Thermal structure of the Anadarko Basin: American Association of Petroleum Geologists Bulletin, v. 83, p. 333-361.

Hamilton, Wayne, 1987, Crustal extension in the Basin and Range province, southwestern United States, *in* Coward, M.P., Dewey, J.F., and Hancock, P.L., editors, Continental Extensional Tectonics: London, Geological Society Special Publication, v. 28, p. 155-176.

Hintze, L.F., 1988, Geologic history of Utah: Provo, Utah, Brigham Young University, Brigham Young University Geology Studies Special Publication no. 7, 202 p.

Hodge, D.S., Hilfiker, K.G., De Rito, R.F., Maxwell, J.R., Morgan, Paul, and Swanberg, C.A., 1980, Relationship of heat flow and temperature gradients to basement lithology: Eos Transactions of the American Geophysical Union, v. 61, p. 363.

Horner, D.R., 1951, Pressure buildup in wells: Proceedings of the World Petroleum Congress, v. 3rd (2), p. 503-521.

Hunt, C.B., 1956, Cenozoic geology of the Colorado Plateau: United States Geological Survey Professional Paper 279, 99 p.

Jarrard, R.D., Erickson, S. N., Sondergeld, C.H., Chan, M.A., and Kayen, R.E., 1999, Sandstone exhumation effects on velocity and porosity: Perspectives from the Ferron sandstone, manuscript in preparation.

Keho, T.H., 1987, Heat flow in the Uinta Basin: Salt Lake City, University of Utah, M.S. thesis, 99 p.

Keller, G.R., Smith, R.S., Braile, L.W., Heaney, R.J., and Shurbet, D.H., 1979, Upper crustal structure of the eastern Basin and Range, northern Colorado Plateau and Middle Rocky Mountains from Rayleigh wave dispersions: Bulletin of the Seismological Society of America., v. 66, p. 869-876.

Klemperer, S.L., Hauge, T.A., Hauser, E.C., Oliver, J.E., and Potter, C.J., 1986, The Moho in the northern Basin and Range province, Nevada, along the COCORP 40°N seismic-reflection transect: Bulletin of the Geological Society of America, v. 97, p. 603-618.

Lachenbruch, A.H., 1968, Rapid estimation of the topographic disturbances to superficial thermal gradients: Reviews in Geophysics, v. 6, p. 365-400.

— 1978, Heat flow in the Basin and Range province and thermal effects of tectonic extension: Pure Applied Geophysics, v. 117, p. 34-50.

Lachenbruch, A.H., and Brewer, M.C., 1959, Dissipation of the thermal effect of drilling a well in arctic Alaska, U.S. Geological Survey Bulletin 1083-C,

Lachenbruch, A.H., Sass, J.H., Munroe, R.J., and Moses, T.H., Jr., 1976, Geothermal setting and simple heat conduction models for the Long Valley Caldera: Journal of Geophysical Research, v. 81, p. 769-784.

Lachenbruch, A.H., Sass, J.H., and Morgan, Paul, 1994, Thermal regime of the southern Basin and Range province; Implications of heat flow for regional extension and metamorphic core complexes: Journal of Geophysical Research, v. 99, p. 22121-22133.

Loeb, D.T., 1986, The P-wave structure of the crust - mantle boundary beneath Utah: Salt Lake City, University of Utah M.S. thesis, 125 p.

Lowry, A.R., and Smith, R.B., 1995, Strength and rheology of the western U.S. Cordillera:

Journal of Geophysical Research, v. 100, p. 17,947-17,963.

Luheshi, M.N., 1983, Estimation of formation temperature from borehole measurements: Geophysical Journal of the Royal Astronomical Society, v. 74, p. 747-776.

McGetchin, T.R., 1979, Introduction to special issue, plateau uplift - mode and mechanism: Tectonophysics, no. 61, XI-XII,

McGetchin, T.R., Burke, K.C., Thompson, A.B., and Young, R.A., 1980, Mode and mechanism of plateau uplift, *in* Bally, A.W., Bender, P.L., McGetchin, T.R. and Walcott, R.I., editors, Dynamics of plate interiors: Washington, D.C., American Geophysical Union Geodynamic Series v. 1, p. 99-110.

Moran, K.J., 1991, Shallow thermal regime at the Jordanelle dam site, central Rocky Mountains, Utah: Salt Lake City, University of Utah, M.S. thesis, 141 p.

Pechmann, J.C., Nava, S.J., and Arabasz, W.J., 1992, Seismological analysis of four recent moderate (4.8 to 5.4) earthquakes in Utah: Utah Geological Survey, Contract Report 92-1, 107 p.

Powell, W.G., 1997, Thermal state Colorado Plateau-Basin and Range transition, Salt Lake City, University of Utah, Ph.D. thesis, 232 p.

Powell, W.G., and Chapman, D.S., 1990, A detailed study of the heat flow at the Fifth Water site, Utah, in the Basin and Range - Colorado Plateau transition, Tectonophysics, v. 176, p. 291-314.

Powell, W.G., Chapman, D.S., Balling, Niels, and Beck, A.E., 1988, Continental heat flow density, *in* Haenel, R., Rybach, Ladislaus, and Stegena, Lajos, editors, Handbook of terrestrial heat-flow density determination: Kluwer Academic Publishers, p. 167-222.

Reiter, Marshall, and Mansure, A.J., 1982, Geothermal studies in the San Juan Basin and the Four Corners area of the Colorado Plateau I - terrestrial heat-flow measurements: Tectonophysics, v. 91, p. 233-251.

Reiter, Marshall, Mansure, A.J., and Shearer, C.F., 1979, Geothermal characteristics of the Colorado Plateau: Tectonophysics, v. 61, p. 183-195.

Reiter, Marshall, and Tovar, J.C., 1982, Estimates of terrestrial heat flow in northern Chihuahua, Mexico, based on petroleum bottom hole temperatures: Bulletin of the Geological Society of America, v. 93, p. 613-624.

Roy, R.F., Blackwell, D.D., and Birch, F.S., 1968, Heat generation of plutonic rocks and continental heat flow provinces: Earth and Planetary Science Letters, v. 5, p. 1-12.

Roy, R.F., Decker, E.R., Blackwell, D.D., and Birch, F.S., 1968, Heat flow in the United States: Journal of Geophysical Research, v. 73, p. 5207-5221.

Rybach, Ladislaus, 1986, Amount and significance of radioactive heat sources in sediments, *in* Burrus, Jean, editor, Thermal Modeling in Sedimentary Basins: Paris, Technip, 311- 322 p.

Sass, J.H., Kennelly, J.P., Jr., Smith, E.P., and Wendt, W.E., 1984, Laboratory line-source methods for the measurement of thermal conductivity of rocks near room temperature, United State Geological Survey Open File Report, no. 84-91, 21 p.

Sass, J.H., Lachenbruch, A.H., and Munroe, R.J., 1971a, Thermal conductivity of rocks from measurements on fragments and its application to heat flow determinations: Journal of Geophysical Research, v. 76, p. 3391-3401.

Sass, J.H., Lachenbruch, A.H., Munroe, R. J., Greene, G.W., and Moses, T.H. Jr., 1971b, Heat flow in the western United States: Journal of Geophysical Research, v. 76, p. 6376-6413.

Sbar, M.L., and Sykes, L.R., 1973, Contemporary compressive stress and seismicity in eastern North America, and examples of intraplate tectonics: Bulletin of the Geological Society of America., v. 84, p. 1861-1882.

Sclater, J.G., and Christie, P.A.F., 1980, Continental stretching: An explanation of the post-Mid-Cretaceous subsidence of the central North Sea Basin: Journal of Geophysical Research, v. 85, p. 3711-3739.

Scott, G. N., 1982, Temperature equilibration in boreholes - a statistical approach: Ann Arbor, University of Michigan, M.S. thesis, 63 p.

Smith, R.B., 1978, Seismicity, crustal structure, and intraplate tectonics of the interior of the western Cordillera, *in* Smith, R.B., and Eaton, G.P., editors, Cenozoic Tectonics and Regional Geophysics of the Western Cordillera: Geological Society of America, no.152, p. 111-144.

Speece, M.A., Bowen, T.D., Folcik, J.L., and Pollack, H.N., 1985, Analysis of temperatures in sedimentary basins - the Michigan Basin: Geophysics, v. 50, p. 1318-1334.

Stokes, W.L., 1986, Geology of Utah: Salt Lake City, Utah, Utah Museum of Natural History, Occasional Paper no. 6, 280 p.

Thompson, G.A., and Zoback, M.L., 1979, Regional geophysics of the Colorado Plateau: Tectonophysics, v. 19, p.149-164.

Touloukian, Y.S., Liley, D.E., and Saxena, S.L., 1970, Thermophysical Properties of Matter, volume 3, thermal conductivity - nonmetallic liquids and gasses: New York Plenun, p.

Willett, S.D., 1988, Spatial variation of the temperature and thermal history of the Uinta Basin, Salt Lake City, University of Utah, Ph.D. thesis, 121p.

Wilson, J.T., 1973, Mantle plumes and plate motions, Tectonophysics, v. 19, p. 149-164.

Wong, I.G., and Humphrey, J.R., 1989, Contemporary seismicity, faulting and the state of stress in the Colorado Plateau, Bulletin of the Geological Society of America, v. 101, p. 1127-1146.

Zoback, M.L., and Zoback, M.D., 1980, State of stress in the conterminous United States: Journal of Geophysical Research, v. 85, p. 6113-6156.

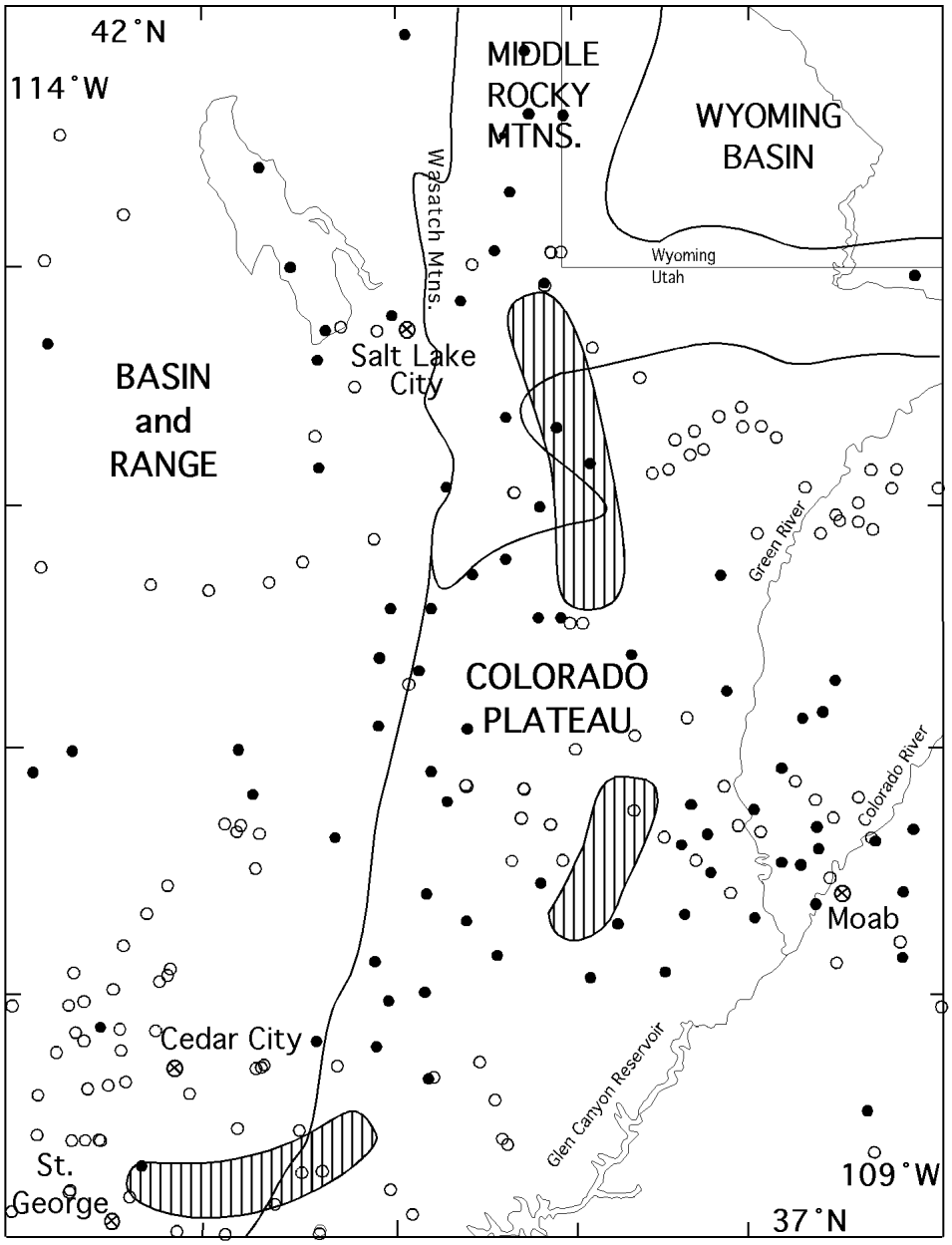

Figure 1. Locations of the new heat flow sites. Solid circles indicate new data, open circles are previously published. Major physiographic boundaries are indicated by fine lines (from Fenneman, 1946). Hatched areas are the thermal transition as defined by Powell (1997).

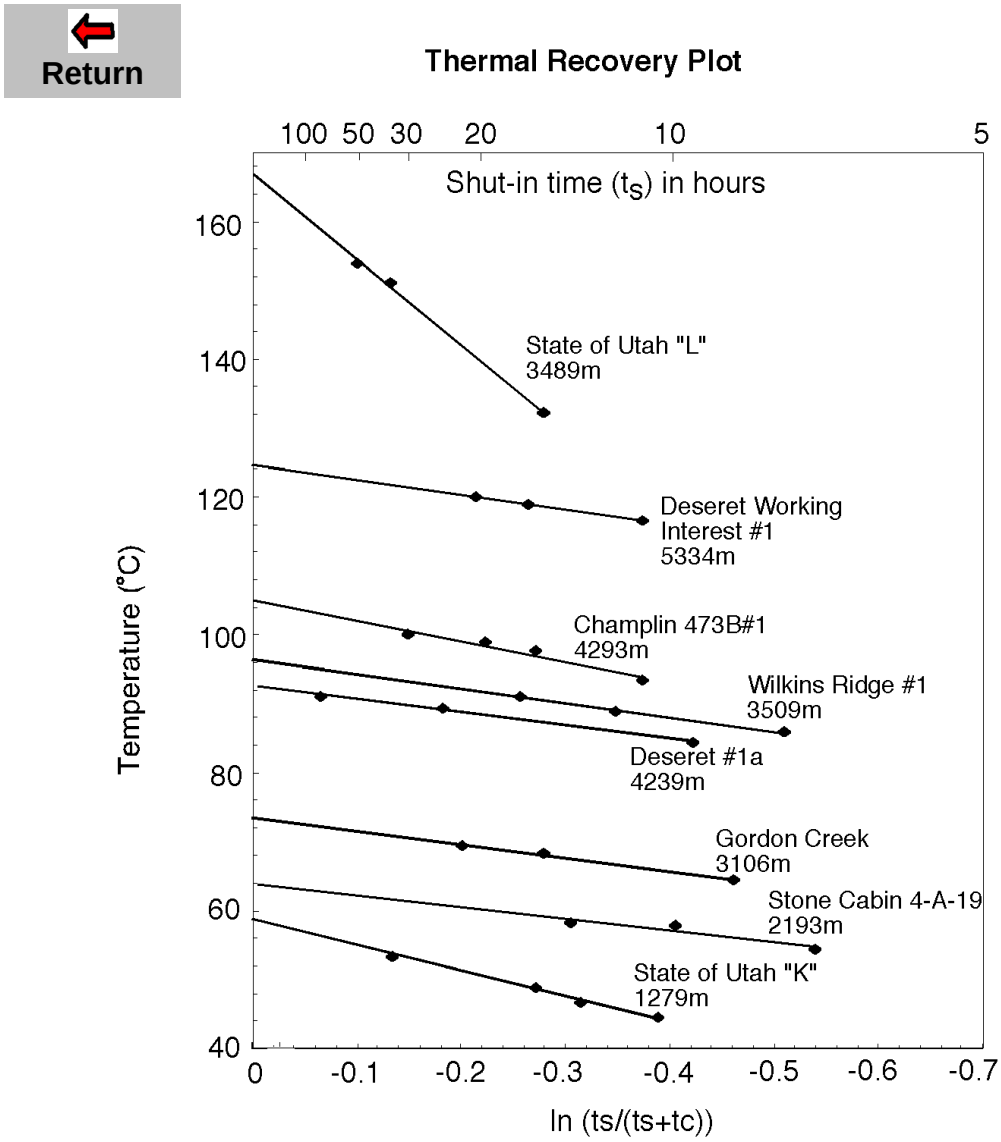

Figure 2. Thermal recovery plot for a representative selection of wells. Various depths and geographical regions are represented. The temperature-intercept of each line indicates the steady-state temperature for that depth in that well.

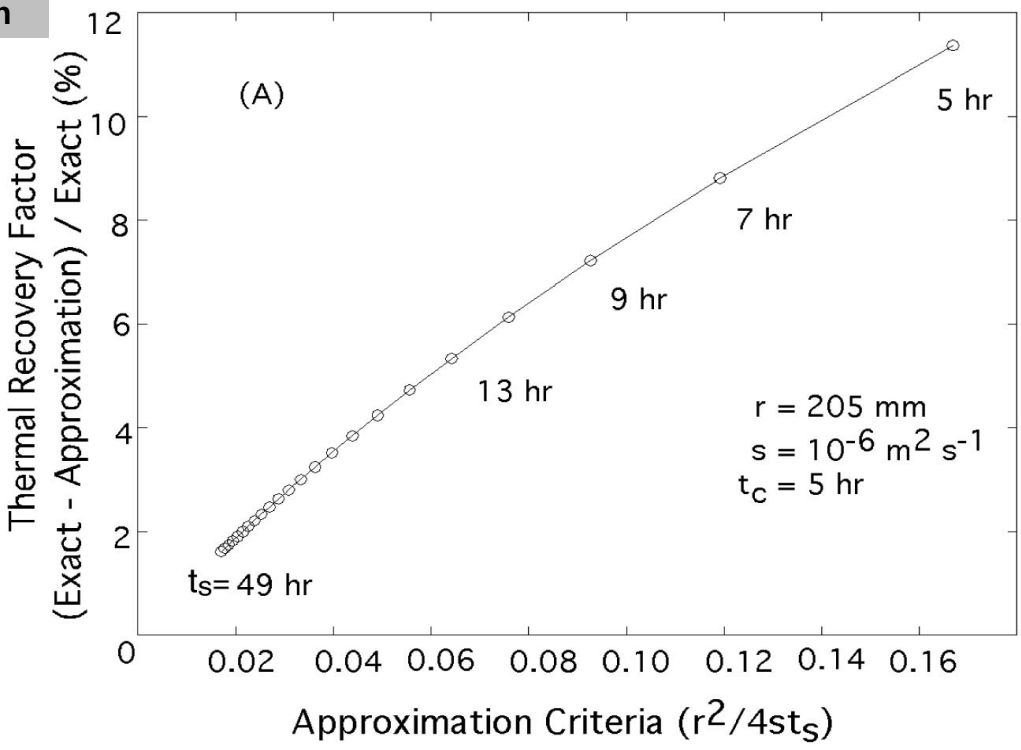

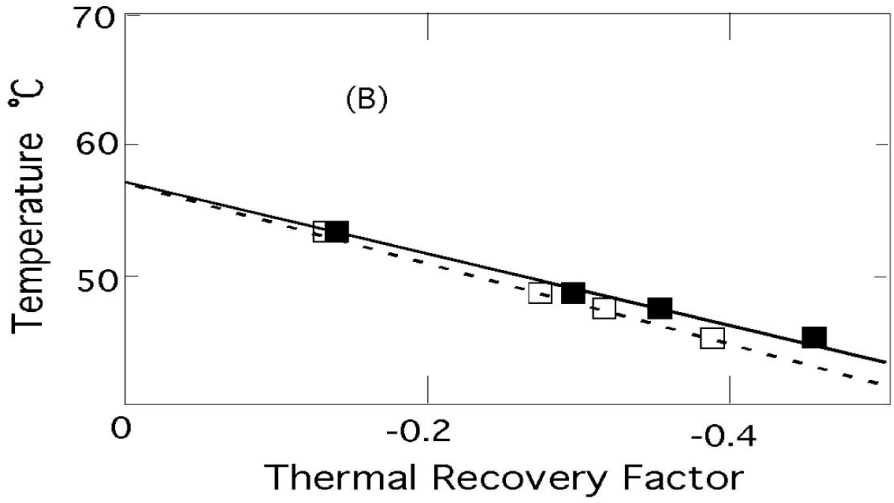

Figure 3. Borehole thermal recovery. (A) shows the difference between the thermal recovery factors of the exact solution and the approximation plotted against the criterion for using the approximation. The approximation criterion is changing with the shut-in times, in this case 5-49 hours in 2 hour intervals. (B) shows the relative insensitivity of calculated steady-state temperature in spite of large differences in thermal recovery factors between the approximation (dashed line, open symbols) and the exact solution (solid line, closed symbols).

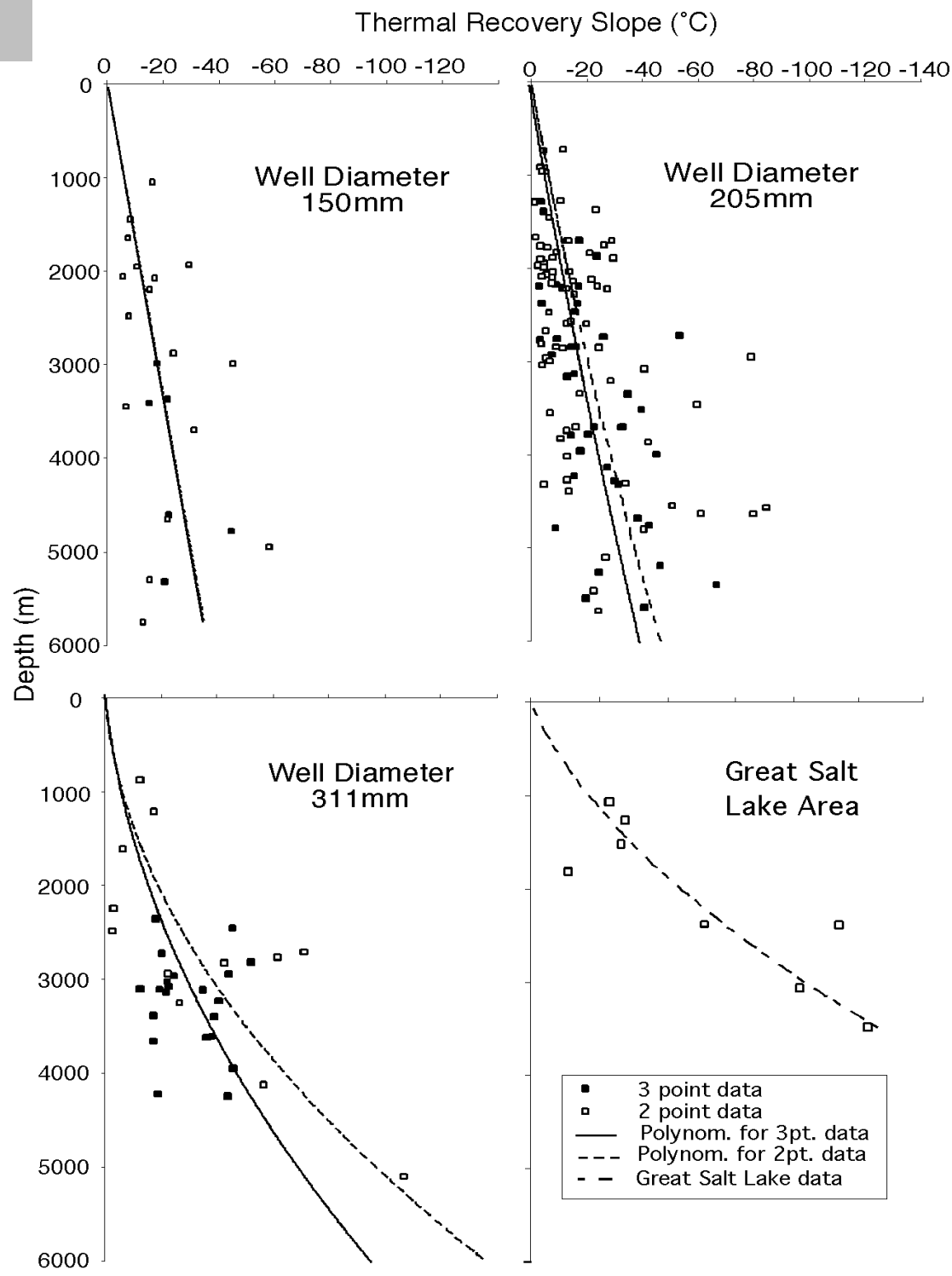

Figure 4. Depth dependence of thermal recovery slopes. The slopes of each thermal recovery plot are plotted as a function of depth with each well diameter group plotted separately. The data from the Great Salt Lake area are plotted as a separate group.

Return

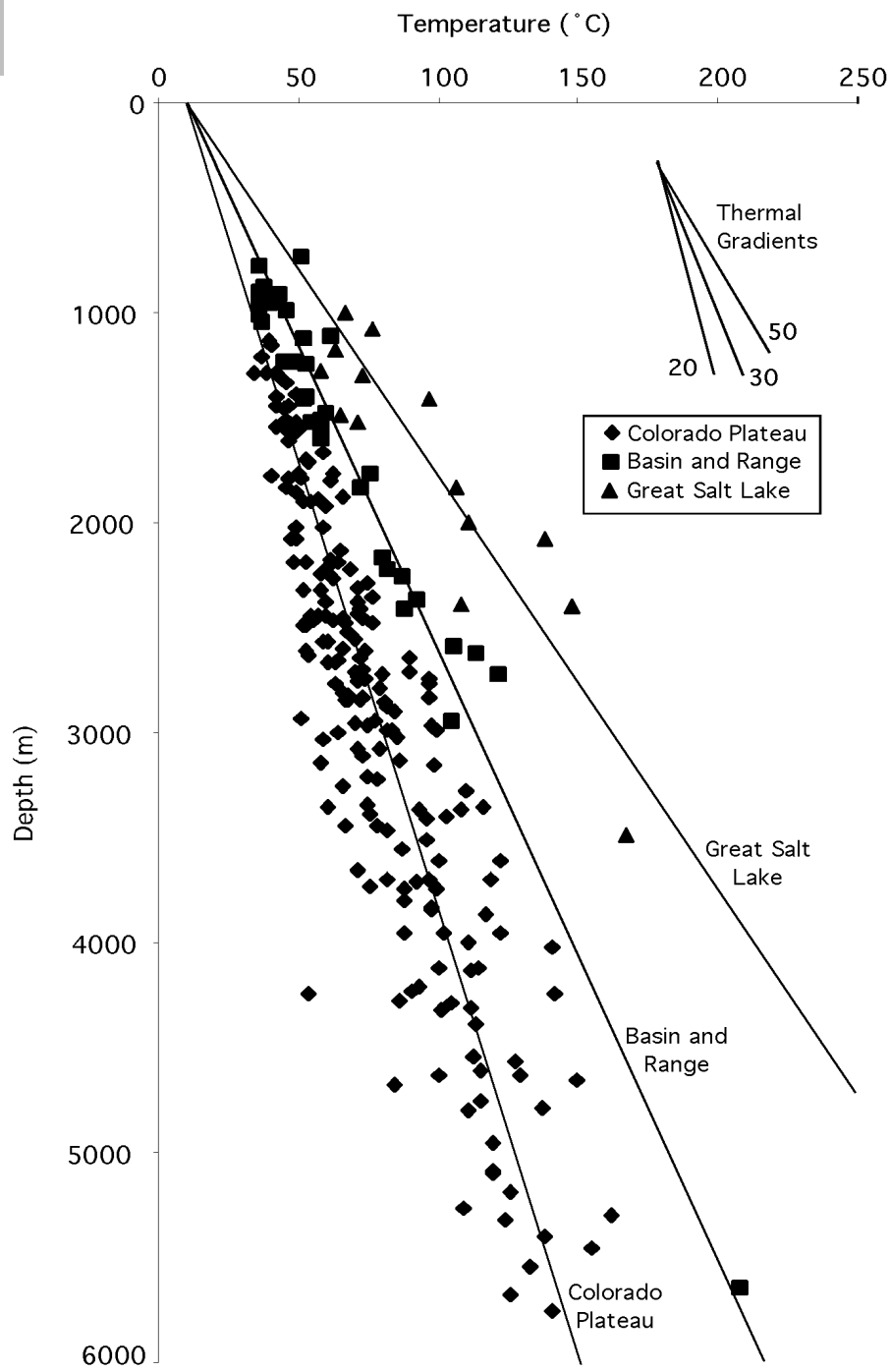

Figure 5. Temperature versus depth for all of the data collected in this study. Average thermal gradients projected on the figure are for the Great Salt Lake (60°C km^{-1}), Basin and Range (35°C km^{-1}) and Colorado Plateau (26°C km^{-1}). The Basin and Range and Colorado Plateau are separated according to the geomorphic transition.

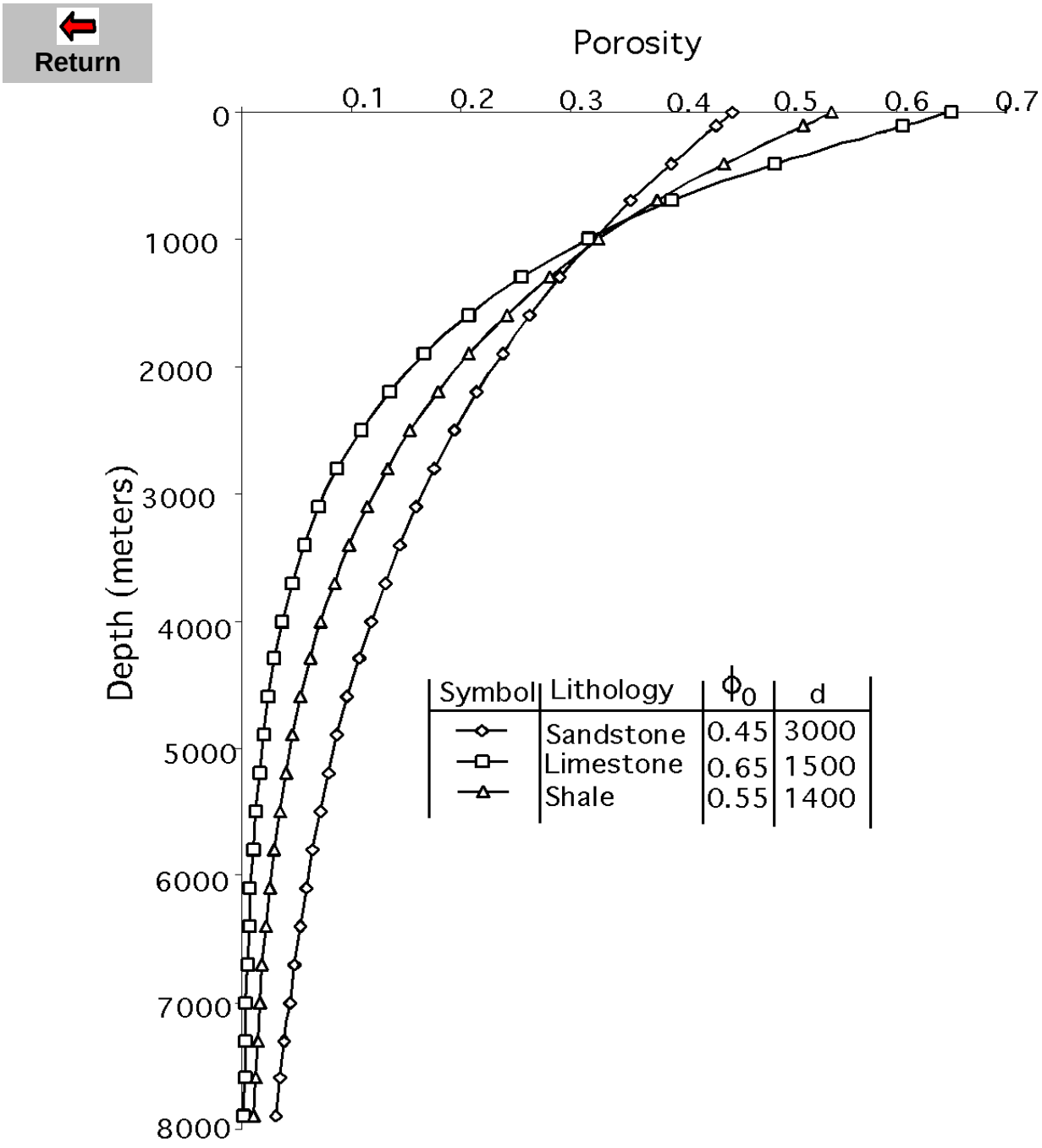

Figure 6. Porosity-depth compaction curves. Three categories of sediments are used to determine porosity and burial-exhumation magnitudes.

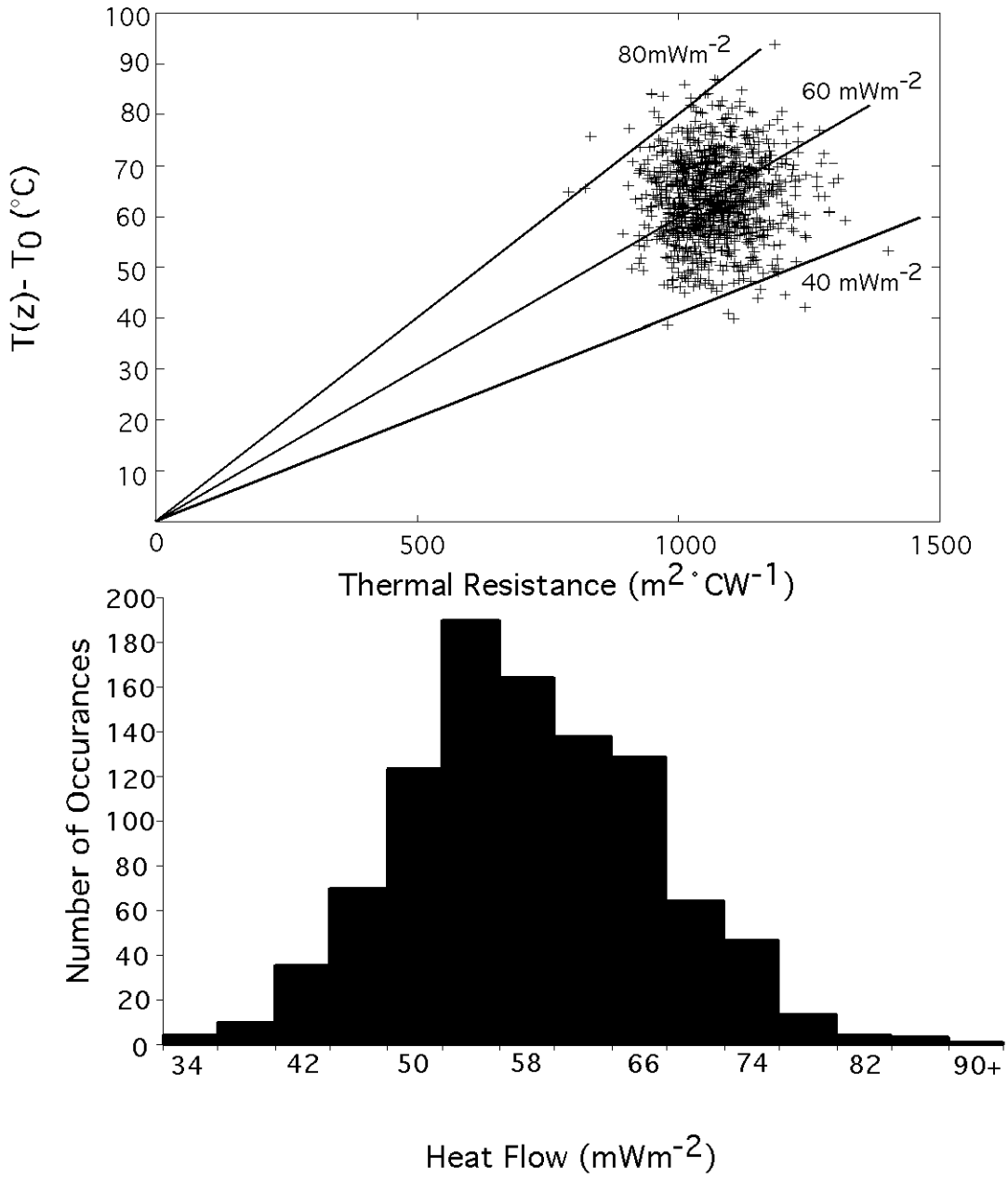

Figure 7. Monte-Carlo analysis for Salt Valley #1 on the Colorado Plateau near Moab, Utah.

Return

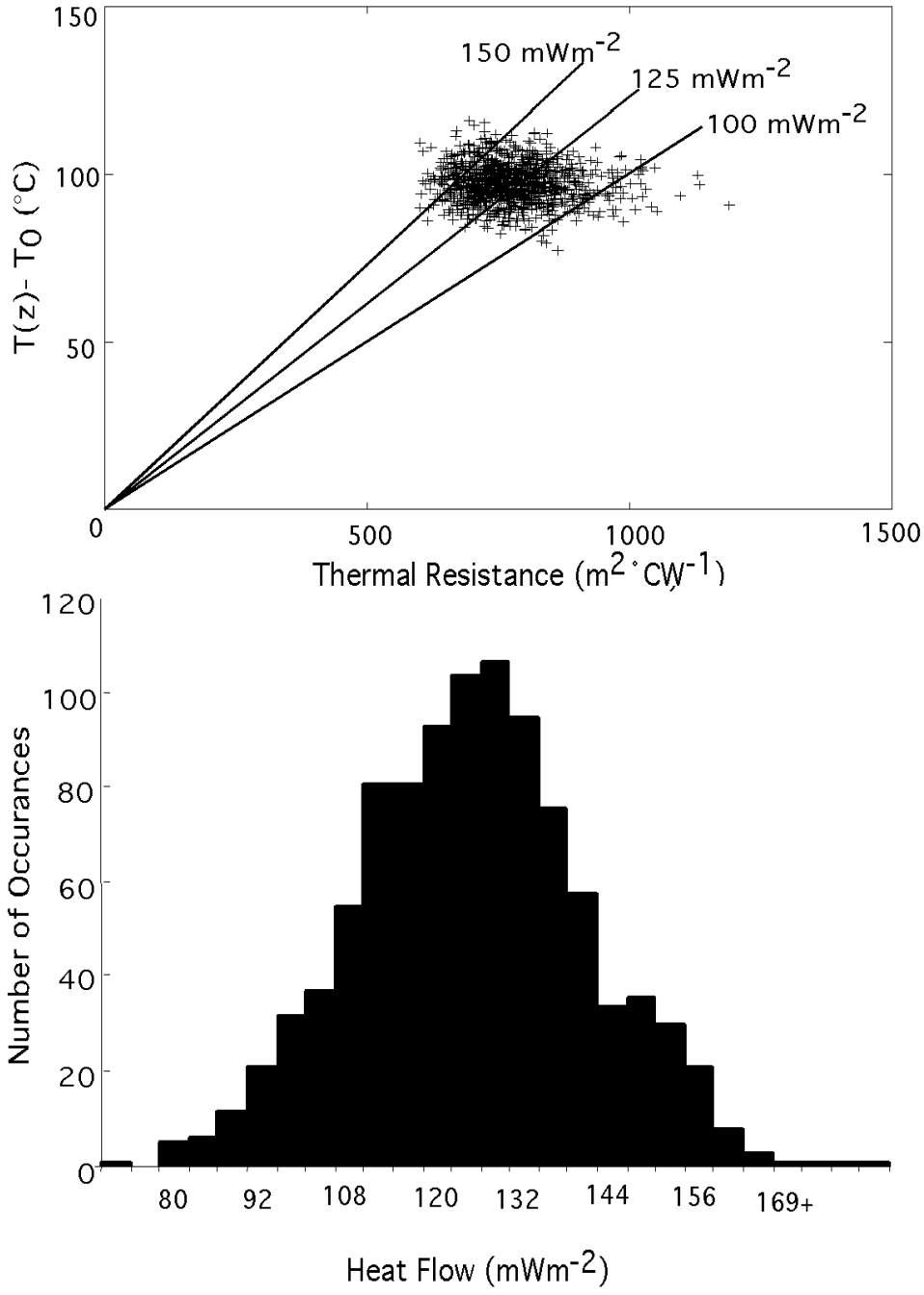

Figure 8. Monte Carlo analysis of "State of Utah N#1" in the Basin and Range, near the Great Salt Lake.

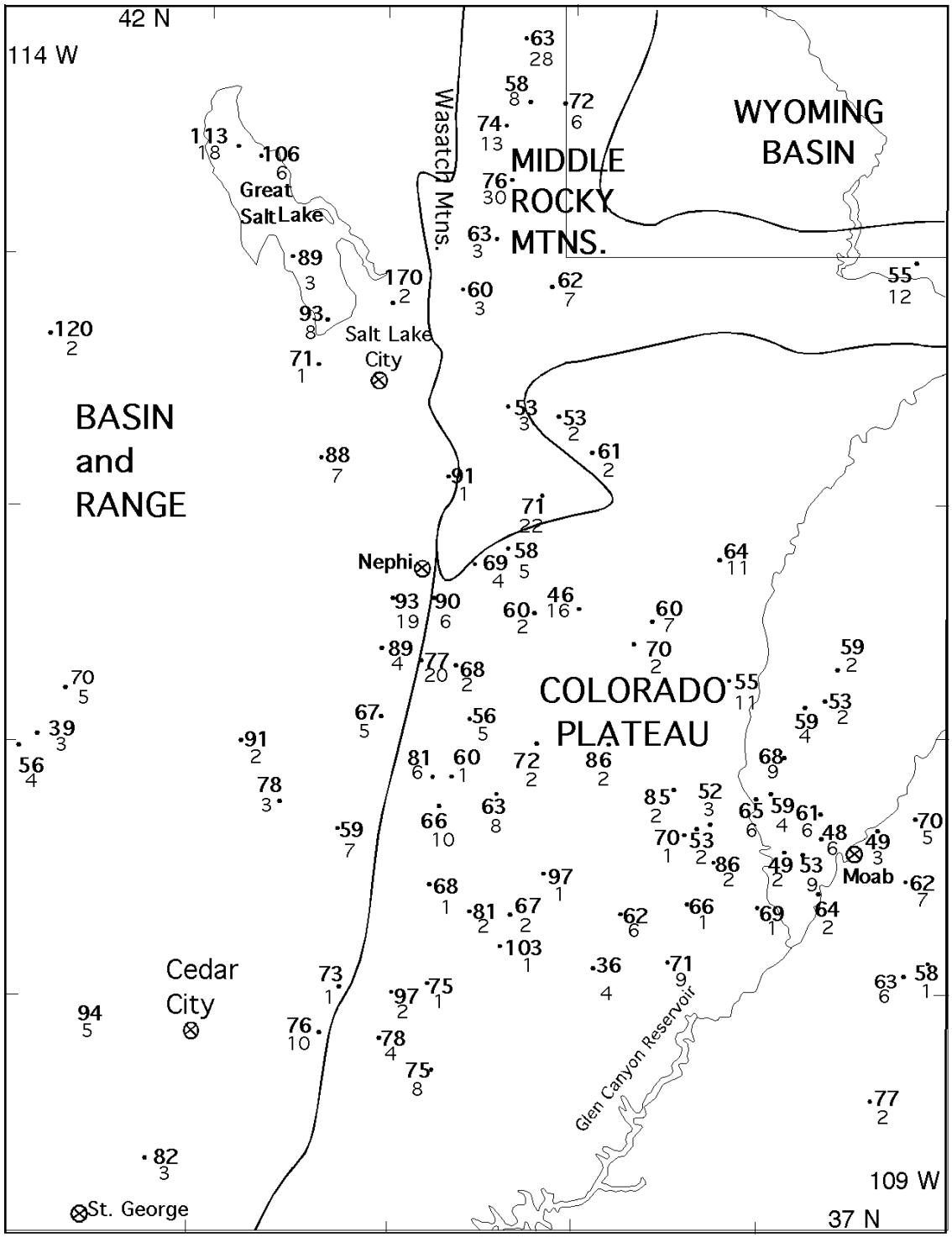

Figure 9. New heat flow values from oil and gas well data. The bold upper numbers are heat flow in mW m^{-2} and the lower numbers represent the number of transient BHTs used in the heat flow calculation.

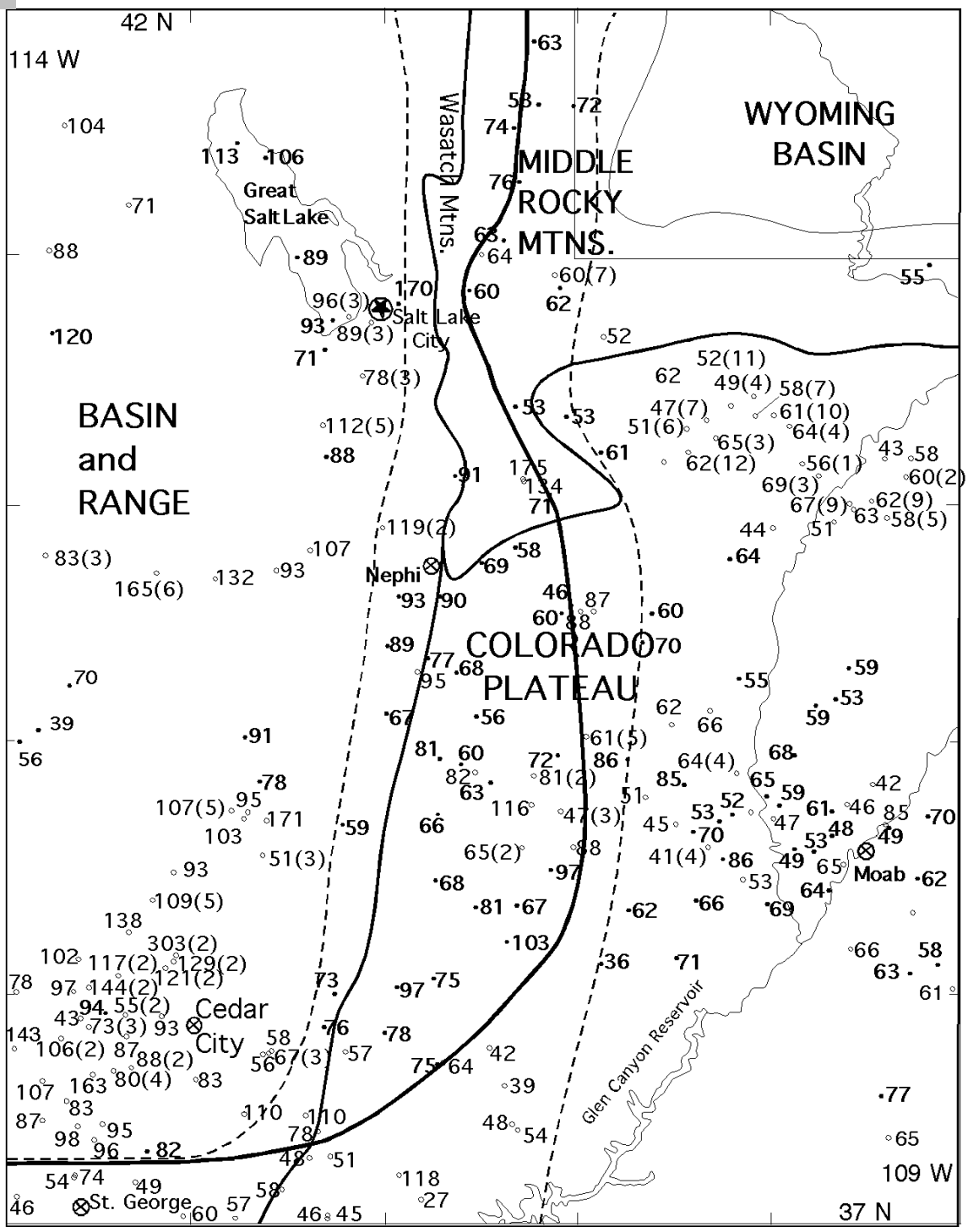

Figure 10. Heat flow data for Utah. The values in bold are from this study, other values are from previous studies and the numbers in parenthesis indicate the number of heat flow values averaged together to facilitate legibility. The thermal transition is shown as a single heavy line. The dashed lines delineate the areas used in the mean heat flow calculations. Values are in milliwatts per square meter.

Return

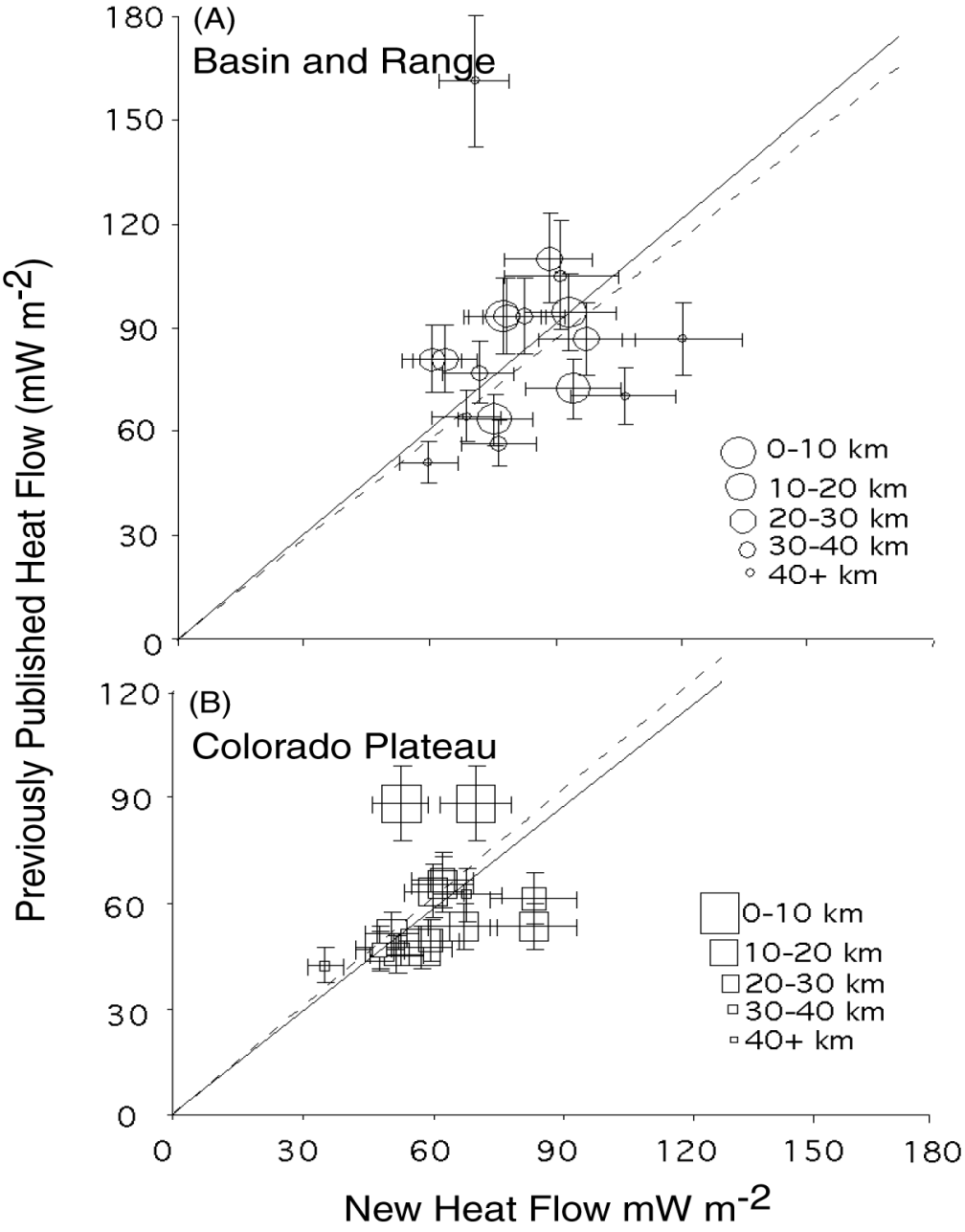

Figure 11. Comparison of new data with nearest-neighbor previously published data. The size of the symbol in the plot indicates the inverse relative distance between two points. The error bars represent the error calculated in the Monte Carlo analyses. The solid line represents the least-squares best-fit line to the data. The dashed line indicates a 1:1 correlation between old and new data.

Return

Table 1. Thermal recovery coefficients.

Well Group	*a* x10 $^{-3}$ °C m^{-1}	*b* x 10^{-6} °C m^{-2}	slope error estimate (%)
150 mm	5.9	0	16
205 mm	6.0	0.2	19
311 mm	4.1	2.0	24
Great Salt Lake	1.5	6.0	25

Coefficients for equations describing the best fit thermal recovery plots, as shown in Figure 4. The slope error is the quotient of the standard deviation of the slopes used to calculate the coefficients and the average slope.

Return

Table 2. Results of rms residual for thermal recovery slopes.

Well Group	2 datapoint mean rms residual (°C)	3 or more datapoint mean rms residual (°C)	all data mean rms residual (°C)
150 mm	13.7	8.5	12.6
205 mm	16.0	11.9	14.6
311 mm	20.1	17.4	18.4
Great Salt Lake			19.7

The Great Salt Lake data were not included in this analysis because the dataset for the GSL is too small. Note that the higher confidence data have the lower residual.

Return

Table 3. New thermal conductivity and porosity data.

Formation	Lith.	N	Matrix Conductivity (W m $^{-1}$ K $^{-1}$)	Std. Deviation (W m $^{-1}$ K $^{-1}$)	Porosity (%)	Std Deviation n (%)
Hermosa	Sh	9	1.63	0.14		
Hermosa	Ss	5	4.78	0.08	22.0	0.5
Mancos	Sh	24	*1.7			
Simonson	Ls	9	2.91	0.17	2.2	0.96
Sevy	Dol	1	6.41		1.0	
Guilmette	Ls	9	2.46	0.35	10.3	4.18

N is the number of samples measured for each formation.
*The thermal conductivity of the Mancos Shale used in the heat-flow calculations is based on nearest-neighbor field calibration discussed in text.

Return

Table 4. Matrix thermal conductivity of Mancos Shale.

Well name	Thermal Conductivity[1]	Mancos Shale as % of section penetrated	% change[2]
Price Area	2.8	43	17
Federal 41-33	1.7	37	20
Bogart Cyn.	1.3	33	11
Range Creek	2.7	8	16
Federal 1-26	1	7	4
Rattlesnake Cyn.	1.3	49	17
One Eye State	1.4	44	15

1. Matrix conductivity for the Mancos Shale required for the specific well to have heat flow identical to its nearest-neighbors. 2. Percentage change between heat flow calculated using a laboratory average matrix conductivity of 2.48 W $m^{-1}K^{-1}$ and the field calibrated matrix conductivity of 1.7 W $m^{-1}K^{-1}$.

Return

Table 5. Factors in the Monte Carlo error analysis.

Parameter	Factor variability	Typical variability (%)	Typical perturbation
Thermal conductivity (k)	St.dev.of (k)	10	0.3W m^{-1} K^{-1}
Surface temp (T_0)	Instrument error	10	1°C
BHT (T(z))	Instrument error	10	8°C
Depth of layer interfaces	Lithological variability	15	20-150 m